Geochemistry Geophysics Geosystems G3
AN ELECTRONIC JOURNAL OF THE EARTH SCIENCES
Published by AGU and the Geochemical Society

Article
Volume 8, Number 5
30 May 2007
Q05N12, doi:10.1029/2006GC001514
ISSN: 1525-2027

Low-latitude hydrological cycle and rapid climate changes during the last deglaciation

Camille Levi
LSCE/IPSL, Laboratoire CNRS/CEA/UVSQ, Domaine du CNRS, F-91198 Gif-sur-Yvette, France

Lamont-Doherty Earth Observatory of Columbia University, 61 Route 9W, Palisades, New York 10964, USA

Laurent Labeyrie
LSCE/IPSL, Laboratoire CNRS/CEA/UVSQ, Domaine du CNRS, F-91198 Gif-sur-Yvette, France

Institut Universitaire de France, Université Versailles St-Quentin, Versailles, France

Franck Bassinot, François Guichard, Elsa Cortijo, Claire Waelbroeck, and Nicolas Caillon
LSCE/IPSL, Laboratoire CNRS/CEA/UVSQ, Domaine du CNRS, Gif-sur-Yvette, F-91198 France (clairew@lsce.cnrs-gif.fr)

Josette Duprat
EPOC, Université Bordeaux 1, Avenue des Facultés, F-33405 Talence Cedex, France

Thibault de Garidel-Thoron
CEREGE, Aix-Marseille Université, CNRS, F-13545 Aix-en-Provence, France

Harry Elderfield
Department of Earth Sciences, University of Cambridge, Downing Street, Cambridge CB2 3RQ, UK

[1] Sea surface temperature and oxygen isotopic records from two well-dated Indian Ocean cores covering the last deglaciation show the occurrence of two periods of increased salinity along the route of warm surface water transport from the Indian to the Atlantic Ocean, one between 18 and 14.5 ka and the other during the Younger Dryas. Our results imply that during these periods, salt accumulated in the tropical Atlantic, creating favorable conditions for an abrupt resumption of the thermohaline circulation and abrupt northern hemisphere warming. Furthermore, we suggest that the observed pattern of millennial climate variability during the last glacial and deglaciation resulted from the interaction between the relatively slow rhythm of expansion and decay of the northern hemisphere ice sheets, and El Niño–Southern Oscillation variability, through changes in the position of the Intertropical Convergence Zone. This interaction generated an oscillator with millennial time response that operated at times of sufficient northern hemisphere ice sheets extent.

Components: 6780 words, 4 figures.

Keywords: rapid climate changes; low-latitude hydrological cycle; last deglaciation.

Index Terms: 4999 Paleoceanography: General or miscellaneous; 1605 Global Change: Abrupt/rapid climate change (4901, 8408); 4922 Paleoceanography: El Nino (4522).

Received 16 October 2006; **Revised** 29 December 2006; **Accepted** 7 March 2007; **Published** 30 May 2007.

Levi, C., L. Labeyrie, F. Bassinot, F. Guichard, E. Cortijo, C. Waelbroeck, N. Caillon, J. Duprat, T. de Garidel-Thoron, and H. Elderfield (2007), Low-latitude hydrological cycle and rapid climate changes during the last deglaciation, *Geochem. Geophys. Geosyst.*, *8*, Q05N12, doi:10.1029/2006GC001514.

Theme: Past Ocean Circulation

1. Introduction

[2] Millennial scale climate variability observed during the last glacial period characterized by Heinrich events and Dansgaard-Oeschger cycles [*Bond et al.*, 1992, 1993; *Heinrich*, 1988] has been mostly attributed to high-latitude interactions between atmosphere, ice and ocean [*Broecker*, 1994]. However, recent studies have suggested that low-latitude climatology may play a major role in this variability [e.g., *Cane and Clement*, 1999; *Clement et al.*, 1999; *Peterson et al.*, 2000]. The importance of low-latitudes in global climate can be readily seen from the fact that tropical warming leads polar ice melting and high northern latitude warming at both glacial-interglacial [*Hays et al.*, 1976] and millennial scales [*Lea et al.*, 2000; *Rühlemann et al.*, 1999; *Schmidt et al.*, 2004; *Visser et al.*, 2003]. Yet, a thorough understanding of past changes in tropical climatology and connections with global climate variability is still lacking.

[3] Low latitudes are a major source of latent heat transferred to the atmosphere. Several recent studies have concluded that large changes in hydrological cycles analogous to those associated to El Niño–Southern Oscillation (ENSO) could be a dominant feature of the tropical Pacific and Indian oceans over glacial-interglacial and millennial scales [*Cane and Clement*, 1999; *Clement et al.*, 1999; *Palmer and Pearson*, 2003; *Stott et al.*, 2002]. El Niño is understood to be one phase of a natural mode of oscillation (La Niña is the complementary phase) that results from unstable interactions between the tropical Pacific Ocean and the atmosphere in the modern climate [*Philander*, 1990]. El Niño events occur every three to seven years. During El Niño events, the warm waters and the center of atmospheric convection move eastward from near Indonesia to the vicinity of the dateline. The effects are felt worldwide because the tropical Pacific is a powerful source of heat driving atmospheric circulation. The relatively uniform sea surface temperatures in the tropical Pacific during El Niño are associated with a southward shift of the ITCZ (and northward shift of the South Pacific Convergence Zone) which induce rainfall variations: there is heavy rainfall in central and east equatorial Pacific regions but droughts in the western region covering Indonesia, the Philippines, Hawaii, eastern Australia, as well as in southeastern Africa [*Philander*, 1990; *Ropelewski and Halpert*, 1987]. Modern salinity anomalies (evaporation excess) observed during El Niño events in the Atlantic and Indo-Pacific oceans are shown in Figure 1. A dominant El Niño mode has been hypothesized by [*Stott et al.*, 2002] in the western tropical Pacific during Dansgaard-Oeschger (D-O) stadials. Simultaneous changes in the transport of water vapor in the atmosphere and salt in the upper ocean would impact on ice sheets budget and ocean circulation, and hence on global climate conditions. Few studies, however, have addressed the role of this meridional transport of water vapor and oceanic salt in global climate changes. To explore this issue, we document changes in sea surface temperature and salinity obtained from planktonic paleoproxies in two Indian Ocean cores covering the last deglaciation period.

2. Material and Methods

[4] IMAGES sediment core MD98-2165 (9°38.96 S, 118°20.31 E, 2100 m water depth), was retrieved south of the Indonesian archipelago (Figure 1). With a sedimentation rate between 7 and 50 cm ky^{-1}, this core is well suited to monitor rapid climate changes of the tropical Indonesian area. It is located at the present southern limit of the area affected by the fresh water input linked to the monsoon, and thus ideally located to monitor its variability.

[5] 20 accelerated mass spectrometry ^{14}C dates were obtained on core MD98-2165 mono-specific *Globigerinoides ruber* (white) samples. Calendar ages were computed using the CALIB4.3 software [*Stuiver and Braziunas*, 1993] and 1998 marine calibration curve [*Stuiver et al.*, 1998]. Core MD98-2165 age scale was derived by linear inter-

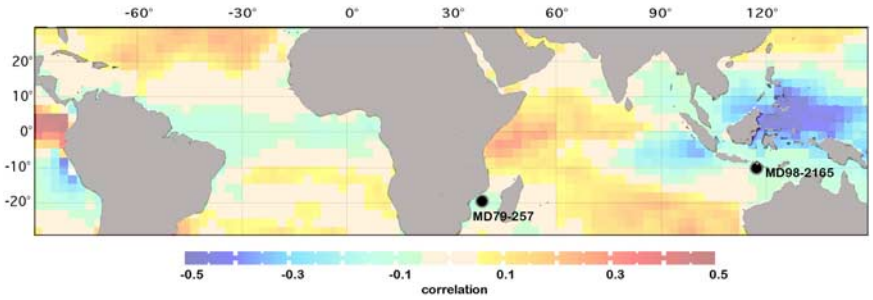

Figure 1. Regression map of NINO3 index (NCEP-NCAR SST anomaly averaged over 150–90°W and 5°S–5°N) versus precipitation minus evaporation (GPCP-NASA data) for the 1979–2001 interval, and location of the studied cores.

polation between the computed calendar ages (Figure 2). The complete table of dated levels and a full description of the age model are given by *Waelbroeck et al.* [2006].

[6] Core MD79-257 (20°24′S, 36°20′E, 1262 m water depth) was retrieved in the Mozambique Channel, on the pathway of Indian tropical upper waters toward the Agulhas current. It is thus well located to monitor the transport of Indian warm surface waters to the Atlantic Ocean. Its sedimentation rate of 13 to 70 cm ky^{-1}, allows high-resolution climate reconstruction. Core MD79-257 has been previously precisely dated [*Duplessy et al.*, 1991]. Since then, 11 additional ^{14}C ages have been measured at LSCE (see auxiliary material[1] Tables S1 and S2) As for core MD98-2165, ^{14}C ages were converted to calendar ages using the CALIB4.3 software and 1998 marine calibration curve [*Stuiver and Braziunas*, 1993; *Stuiver et al.*, 1998]. Sedimentation is not as regular as in core MD98-2165, with a non-erosive turbidite between 115 and 225 cm, and a plateau of constant ^{14}C ages between 500 and 550 cm depth. We thus developed an age model using a polynomial regression of order 6 (Figure 2).

2.1. Isotopic Measurements

[7] Planktonic foraminiferal specimens of *G. ruber* (white) sensu stricto (as defined by *Wang* [2000]) were hand picked in relatively narrow size ranges to minimize size effect on isotopic ratios [*Waelbroeck et al.*, 2005]. For core MD98-2165 *G. ruber* were picked in the 250–315 μm size range. For core MD79-257, new measurements were performed in the 200–250 μm size range in order to increase the temporal resolution between 10 and 18 calendar ky BP (ka) with respect to the published *G. ruber* oxygen isotopic record [*Duplessy et al.*, 1991].

[8] Isotopic measurements were performed, following the standard procedure, at LSCE on Finnigan MAT251 and Delta+ mass-spectrometers. Samples comprised 4 to 14 shells. Data are presented in standard delta notation as the per mil (‰) difference from the Pee Dee Belemnite (PDB) standard. δ^{18}O data are calibrated with respect to NBS19 [*Coplen*, 1988; *Ostermann and Curry*, 2000]. The mean external reproductibility (1σ) of carbonate standards is ±0.05 ‰ for δ^{18}O.

2.2. Sea Surface Temperature Reconstruction

[9] Sea surface temperature (SST) was derived from Mg/Ca measurements on *G. ruber* (white) in core MD98-2165 and from planktonic foraminifera abundances in core MD79-257.

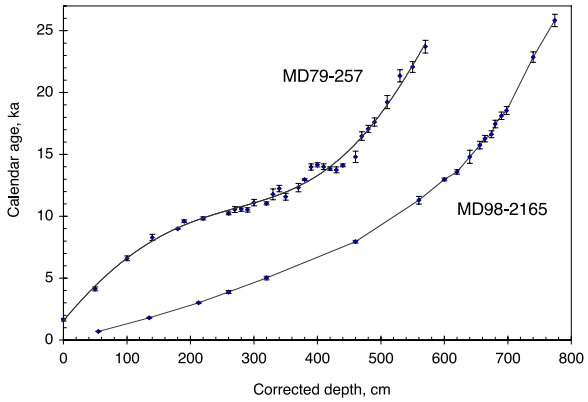

Figure 2. Age-depth relationships for cores MD98-2165 and MD79-257. Solid symbols indicate ^{14}C ages converted in calendar age with associated error bars. Gray lines depict the age model chosen, i.e., sixth-order polynomial fit for core MD79-257 and linear interpolation for core MD98-2165.

[1]Auxiliary material are available at ftp://ftp.agu.org/apend/gc/2006gc001514.

[10] Mg/Ca analyses were performed on adjacent 2-cm samples from 580 to 900 cm (2 cm thickness), and every 10-cm interval (1 cm thickness) from 0 to 580 cm. Samples of 20 specimens of *G. ruber* were cleaned following the method described by Barker and colleagues [*Barker et al.*, 2003] to eliminate contamination from clays and organic matter. Analyses were performed on a Varian Vista Pro Inductively Coupled Plasma Optical Emission Spectrometer (ICP-OES) following the procedure of *de Villiers et al.* [2002]. Precision for measured Mg/Ca ratios determined from replicate runs of a standard solution of Mg/Ca = 5.23 mmol/mol is 0.4% (relative standard deviation (RSD)). Precision for *G. ruber* samples is 4.0% (pooled RSD). Part of the measurements were performed in Cambridge with a slightly less aggressive cleaning method [*Levi*, 2003]. A systematic correction of −0.3 mmol/mol has been applied for alignment with the measurements made at LSCE. Intercalibration between Cambridge and LSCE allows us to exclude problems related to standards.

[11] Derivation of SST from Mg/Ca ratio may be biased if foraminiferal shells have undergone partial dissolution [*Brown and Elderfield*, 1996; *Dekens et al.*, 2002; *Rosenthal and Lohmann*, 2002]. Core MD98-2165 is located above modern and glacial lysocline depth [*Martinez et al.*, 1998] and good calcite preservation is attested by the presence of aragonite throughout the core. Absence of silicate contamination was controlled by measuring Fe, Al and Mn content, with a maximum allowed Fe/Mg ratio of 0.1 mol.mol-1 for high Mg/Ca samples. No sample was rejected. Plotting Mg/Ca against Al/Ca (or Fe/Ca) does not show any outlier that would indicate detrital contamination. Maximum contribution of Mg from Mn-Fe-oxide is about 1% (given the Mg/Mn ratio of about 0.1 mol/mol in nodules and micro nodules [see *Barker et al.*, 2003, and references therein]. Mg/Ca values were converted into SST following [*Dekens et al.*, 2002]: Mg/Ca(mmol/mol) = 0.38 * exp (0.09*SST(°C)).

[12] Core MD79-257 planktonic foraminifera were counted every 10 cm following the methodology and species classification of CLIMAP [*CLIMAP Project Members*, 1981] (except for the class p.d. intergrade which was lumped with *Neogloboquadrina pachyderma* right coiling), with a minimum of 350 individual shells counted in the >150 μm size range at each level. SST was reconstructed from planktonic foraminifera species distribution using the Modern Analog Technique [*Prell*, 1985] and a database of 245 core tops from the south hemisphere [*Salvignac*, 1998]. Reliability of the reconstruction is high as the computed dissimilarity coefficient remains low (mean value = 0.012, 1 sigma = 0.005), average uncertainty on reconstructed winter and summer SST is 1.5°C and 0.7 °C, respectively.

2.3. Sea Surface Salinity Estimate

[13] Sea surface salinity (SSS) is expressed as the local seawater $\delta^{18}O$ anomaly, $\Delta\delta^{18}O_{sw}$. Seawater $\delta^{18}O$ ($\delta^{18}O_{sw}$) depends on changes in local seawater $\delta^{18}O$ and in mean ocean $\delta^{18}O$ resulting from changes in continental ice volume. We extract $\delta^{18}O_{sw}$ from the paleotemperature equation of *Shackleton* [1974]. Local $\Delta\delta^{18}O_{sw}$ changes are then obtained by subtraction of the effect of continental ice melting on global seawater $\delta^{18}O$. The latter is assumed to be equal to the deglacial sea level curve of *Lambeck and Chappell* [2001] multiplied by a constant coefficient of 1.1‰/130 m [*Waelbroeck et al.*, 2002]. Local $\Delta\delta^{18}O_{sw}$ is directly related to salinity [*Duplessy et al.*, 1992], with a change in $\Delta\delta^{18}O_{sw}$ = 0.2 ‰ approximately corresponding to 1 psu change in salinity at low latitudes, but we prefer not to convert $\Delta\delta^{18}O_{sw}$ into salinity units in order to avoid introducing an additional source of uncertainty resulting from possible changes in the $\delta^{18}O_{sw}$/salinity relationship in response to ocean circulation and climate changes.

3. Results

3.1. Planktonic $\delta^{18}O$ and SST

[14] The *G. ruber* $\delta^{18}O$ deglaciation signal presents two steps like other planktonic $\delta^{18}O$ deglaciation records from the tropical Indian Ocean [*Duplessy et al.*, 1981; *Stott et al.*, 2002; *Visser et al.*, 2003] (Figure 3). Mozambique Channel core MD79-257 *G. ruber* $\delta^{18}O$ signal lags that of eastern tropical core MD98-2165 (Figure 3).

[15] The isotopic shift recorded in core MD98-2165 between the Last Glacial Maximum (LGM) and Holocene is about 1.7‰. Attributing 1.05 ± 0.1 ‰ to changes in global ice volume [*Duplessy et al.*, 2002; *Schrag et al.*, 2002] leaves 0.65‰ for temperature and/or salinity variations. The calculated Mg/Ca-SST of the most recent samples is equivalent to observed annual mean SST in this region (~28°C) [*Conkright et al.*, 1998]. Mean Holocene Mg/Ca-SST is 27°C, that is 3°C higher than LGM SSTs (Figure 3). This temperature shift

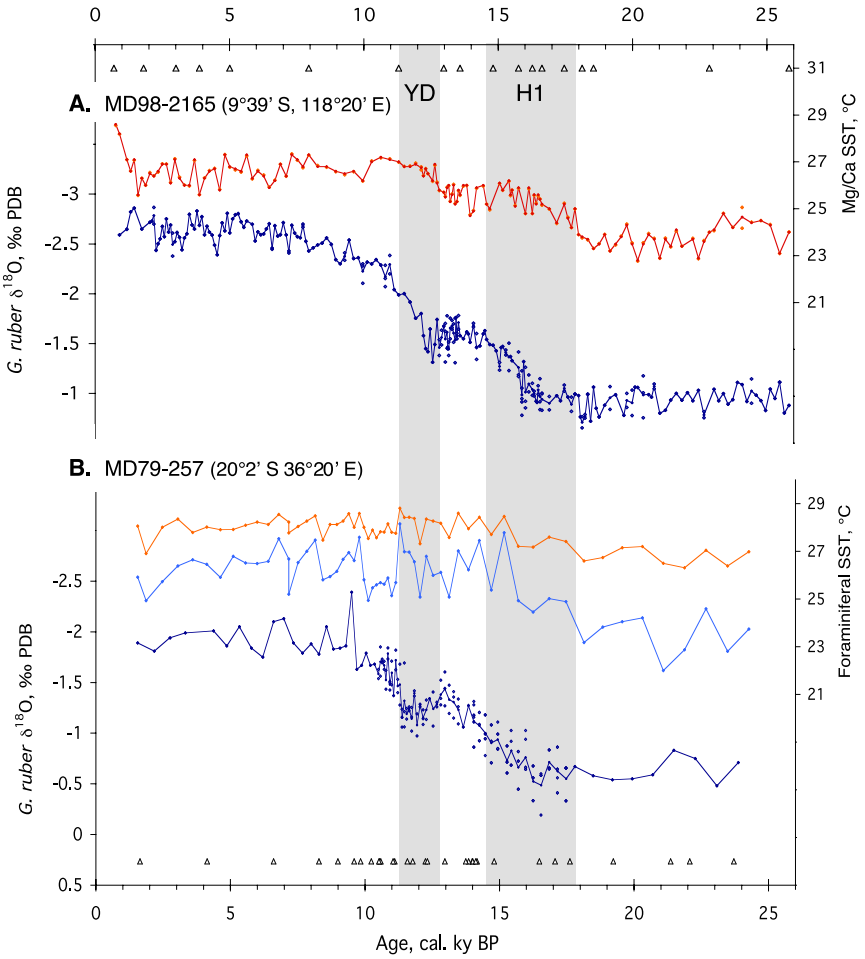

Figure 3. (a) Core MD98-2165 *G. ruber* (white) δ^{18}O and Mg/Ca records versus calendar age. (b) Core MD79-257 *G. ruber* (white) δ^{18}O and foraminiferal summer and winter SST records (obtained using the Modern Analog Technique) versus calendar age. Dots indicate measurement replicates. Lines are drawn through mean values. Empty triangles at the top and bottom of the figure indicate dated levels.

between LGM and Holocene is similar to those found by other authors around Indonesia based on Mg/Ca paleo-thermometry [*de Garidel-Thoron et al.*, 2005; *Lea et al.*, 2000; *Visser et al.*, 2003], but of larger amplitude than the CLIMAP values obtained using foraminifer transfer function [*CLIMAP Project Members*, 1981].

[16] As noted previously in the Indo-Pacific region [*Lea et al.*, 2000; *Rosenthal et al.*, 2003; *Visser et al.*, 2003], SST increase starts around 18.5 ka, synchronously, within the age model resolution, with the warming in Antarctica [*Blunier and Brook*, 2001; *Parrenin et al.*, 2004]. The period 17.5 to 14.5 ka coincides with the cold period associated with Heinrich event 1 in the North Atlantic [*Bond et al.*, 1992, 1993; *Labeyrie et al.*, 1999]. Core MD98-2165 SST increases again during the northern hemisphere cold spell of the Younger Dryas (~13 to 11.6 ka). Between 15 and 13 ka, our SST record documents a slight cooling, at about the time of the Antarctic cold reversal period [*Jouzel et al.*, 1995]. In summary, SST variations between 18.5 and 10 ka seem to be synchronous with central Antarctic ice core temperature changes, as observed in other equatorial western Pacific and Indo-Pacific marine cores [*Lea et al.*, 2000; *Rosenthal et al.*, 2003], as well as in many sites of the eastern equatorial Pacific [*Koutavas et al.*, 2002], Arabian Sea [*Huguet et al.*, 2006], and tropical Atlantic sites [*Rühlemann et al.*, 1999; *Schmidt et al.*, 2004; *Weldeab et al.*, 2006].

[17] SST clearly leads planktonic δ^{18}O changes, both at ~18 ka and ~12.5 ka (Figure 3). This lead is comforted by observed lead of Uk37- and Mg/Ca-SST over planktonic δ^{18}O in other equatorial records

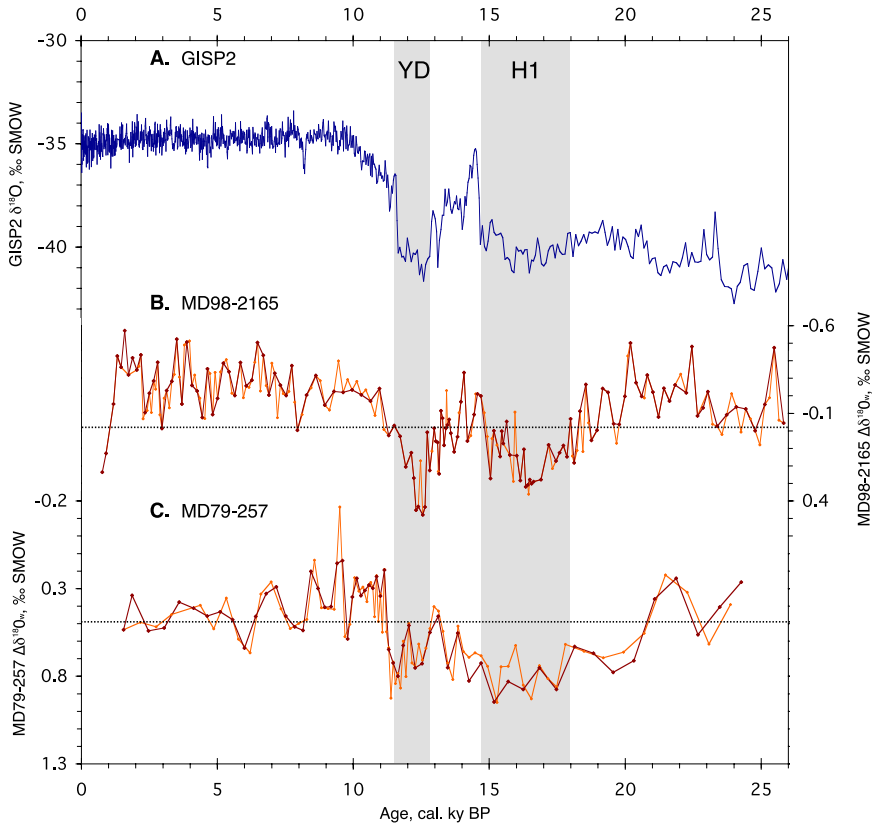

Figure 4. (a) Greenland GISP2 ice $\delta^{18}O$ record [*Alley et al.*, 1993; *Meese et al.*, 1997]. (b) Core MD98-2165 $\Delta\delta^{18}O_{sw}$ computed according to *G. ruber* $\delta^{18}O$ and Mg/Ca sampling. (c) Core MD79-257 $\Delta\delta^{18}O_{sw}$ computed according to *G. ruber* $\delta^{18}O$ and foraminiferal SST sampling.

from equatorial Pacific [*Koutavas et al.*, 2002; *Lea et al.*, 2000], Indo-Pacific area [*Rosenthal et al.*, 2003; *Visser et al.*, 2003], tropical West Indian Ocean [*Bard et al.*, 1997; *Sonzogni et al.*, 1998], and tropical Atlantic [*Rühlemann et al.*, 1999; *Schmidt et al.*, 2004].

[18] Core MD79-257 SST record seems somewhat different from that of core MD98-2165, although the amplitude of the LGM to Holocene warming is similar (Figure 3). It is difficult to precisely compare the two records prior to about 13 ka, as resolution is much lower in core MD79-257. Warming however clearly starts at about 18 ka in both cores. The present foraminiferal SST record is markedly different from the alkenone SST record obtained in the same core [*Bard et al.*, 1997]. First, the deglacial warming starts around 18 ka in our record, whereas it starts around 15.5 ka in the alkenone record. Second, foraminiferal SSTs reach Holocene values by 14 ka, whereas alkenone SSTs slowly increase until 7 ka. Finally, the present record exhibits a clear cooling at the end of the Younger Dryas time interval, from about 11.5 to 10 ka (Figure 3), whereas alkenones indicate a stepwise warming at 11.5 ka [*Bard et al.*, 1997]. However, because alkenones carriers are very light (coccoliths), they are prone to travel long distances and alkenones have been shown to better record transport than SST in areas characterized by vigorous surface currents, such as the Aghulas current [*Sicre et al.*, 2005]. This is why we prefer to use foraminiferal SSTs in the present study, although the time resolution of this record is lower.

3.2. Salinity

[19] Core MD98-2165 and MD79-257 $\Delta\delta^{18}O_{sw}$ records are displayed in Figure 4. The most striking feature is the narrow correspondence between MD98-2165 $\Delta\delta^{18}O_{sw}$ and GISP2 $\delta^{18}O$ between about 18.5 and 10 ka. Heavier $\Delta\delta^{18}O_{sw}$ values correspond to colder temperatures over Greenland, indicating that SSS increases at core MD98-2165 site in phase with temperature decreases over Greenland, and conversely. MD98-2165 SSS is thus relatively high during Heinrich 1 (H1) and the Younger Dryas (YD) and low during the

Bolling-Allerod (B-A) warm event. Moreover, there is no detectable phase lag between MD98-2165 $\Delta\delta^{18}O_{sw}$ and GISP2 $\delta^{18}O$.

[20] The general pattern of core MD79-257 and MD98-2165 $\Delta\delta^{18}O_{sw}$ signals are similar (Figure 4), although sampling resolution of core MD79-257 SST and *G. ruber* $\delta^{18}O$ records prior to ~13 ka is much lower than in core MD98-2165, impeding a detailed comparison of the SSS signals prior to the YD. Also, the end of the salinity increase corresponding to the YD seems to lag the end of the YD recorded in the Greenland ice core by about 300 y. This time lag is however not significant since 300 y is the uncertainty associated with the age model of core MD79-257 at 11.2 ka (Figure 2 and Table S2). A marked $\Delta\delta^{18}O_{sw}$ increase during the YD is clearly visible in core MD79-257, as well as a moderate increase from about 18 to 14.5 ka. SSS thus increased in the Mozambique Channel during H1 and the YD, simultaneously with the SSS increase recorded at core MD98-2165 site.

[21] Within the age models uncertainties, the SSS increases observed in core MD98-2165 and MD79-257 (Figure 4) appear to be synchronous with SSS increases recorded in the tropical western Atlantic, e.g., in Caribbean core VM28-122 [*Schmidt et al.*, 2004].

4. Discussion

4.1. Teleconnections Between Low and High Latitudes

[22] Our SST reconstructions suggest that, compared to the last glacial maximum, a stronger latitudinal temperature gradient may have prevailed during the two stadial periods H1 and YD, with very cold SST at northern high latitudes while we document a warming of 2–3°C in the Indo-Pacific area. An increase of the low- to high-latitude surface temperature gradient acts to enhance the northward transport of moisture by the atmosphere through an intensification of the Hadley circulation cell [*Khodri et al.*, 2001; *Rind*, 2000]. As observed in our cores for H1 and YD, warm SSTs at low latitudes at times of large ice sheets result in more evaporation and could thus induce accelerated growth of the ice sheets [*Kukla et al.*, 2002; *Labeyrie*, 2000], as long as low latitudes warmth lasts. In this scenario, maximum warmth in the tropics would be in phase with increasing ice sheet size and decreasing temperatures at northern high latitudes.

[23] Recent modeling experiments with a coupled atmospheric general circulation and slab ocean model have shown that northern hemisphere ice sheet buildup impacts on atmospheric circulation so as to induce a southward displacement of the Intertropical Convergence Zone (ITCZ) position [*Chiang et al.*, 2003]. This result is consistent with another modeling study using a coupled ocean-atmosphere model showing that a weakening of the Atlantic thermohaline circulation (THC) results in a southward shift of the ITCZ [*Zhang and Delworth*, 2005], and with paleoclimatic data indicating a southward shift of the ITCZ during D-O stadials [*Peterson et al.*, 2000; *Wang et al.*, 2004]. Also, a decrease of East Asian summer monsoon activity is observed in Chinese caves speleothems records during D-O stadials [*Wang et al.*, 2001], which may be explained by a southward shift of the ITCZ associated with the cooling of the Europe-Asia continent. More specifically, there are two categories of SST signals recorded in tropical ocean cores [*Labeyrie et al.*, 2004]: SST records that exhibit the same pattern and timing as Antarctic surface temperature signals [*Rosenthal et al.*, 2003; *Rühlemann et al.*, 1999; *Schmidt et al.*, 2004; *Weldeab et al.*, 2006; this study], and SST records that present the same oscillations as the North Atlantic and Greenland surface temperature signals [*Kienast et al.*, 2001; *Lea et al.*, 2003]. *Labeyrie et al.* [2004] suggest that apparently antagonist changes in tropical Indo-Pacific and Atlantic Ocean cores may reflect regional responses to global, N-S shifts of the ITCZ and associated zonal wind and evaporation/precipitation anomalies.

4.2. Mechanisms at the Origin of Deglaciations and Poststadial Warming at High Northern Latitudes

[24] Results from a three dimensional ocean circulation model show that a gradual warming in the Southern Ocean during deglaciation induces an abrupt resumption of the interglacial mode of the THC, triggered by increased mass transport into the Atlantic Ocean via the warm (Indian Ocean) and cold (Pacific Ocean) water routes [*Knorr and Lohmann*, 2003]. The SSS data from our two Indian Ocean cores further suggest that during the period preceding the B-A, there was an increase in salt transport from the Indian to the Atlantic Ocean, that contributed to the observed accumula-

tion of salt in the tropical Atlantic Ocean [*Schmidt et al.*, 2004].

[25] Accumulated salt in the tropical Atlantic Ocean has been described as a capacitor that could discharge, once the salt quantity is sufficient to counter the influence of meltwater at higher latitudes, inducing an abrupt resumption of the THC [*Paillard and Labeyrie*, 1994; *Schmidt et al.*, 2004]. We postulate here, in agreement with the above modeling results, that, while low salinity polar water and cooling expanded at high northern latitudes during H1, the increase in salinity we observe in the Indian Ocean created favorable conditions for an abrupt resumption of the THC and abrupt northern hemisphere warming at 14.5 ka, i.e., 3 to 4 ky later than the beginning of the gradual warming in the southern hemisphere and global sea level rise.

4.3. Tropical Hydrology

[26] Figure 1 shows that the two studied cores are located in areas (namely the Indonesian archipelago and the Mozambique Channel, off southeastern Africa) which experience sea surface salinity increases during El Niño events. The increase in salinity that we observe during H1 and YD in the two Indian Ocean cores could thus reflect a shift toward an El Niño-like state during stadials, in good agreement with results from *Stott et al.* [2002], who suggested that stadials could correspond to a "super El Niño" mode. Such an El Niño-like state could be either sustained El Niño conditions or an increased frequency of El Niño events resulting in a change in the mean climatic state.

[27] However, it is still unclear why and how the present-day ENSO oscillations would present mode shifts on millennial timescales. A modeling study using a coupled ocean-atmosphere model of the tropical Pacific showed that millennial variability can be generated within the tropics, with or without orbital forcing [*Clement and Cane*, 1999]. *Cane and Clement* [1999] have proposed that global scale millennial variability may be initiated from the tropical Pacific, arguing that the global consequences of changes in the tropical Pacific, which depend on relatively fast atmospheric physics, also operate at longer timescales but did not specify how the climate system would be maintained in an El Niño-like or La Niña-like mode for several centuries.

[28] Here, we suggest that the expansion and decay of northern hemisphere ice sheets over YD, H1 and more generally Dansgaard-Oeschger (D-O) events interacted with ENSO variability through changes in the ITCZ position, hence creating ENSO-like oscillations at millennial timescales. The build up of northern hemisphere ice sheets would be reinforced by dominant El Niño conditions in the tropics as a result of intensified water vapor transport to the high latitudes [*Labeyrie*, 2000; *Rind*, 2000]. Larger northern hemisphere ice sheet extent during northern hemisphere cold events would in turn induce a southward displacement of the ITCZ [*Chiang et al.*, 2003] and a weakening of the Indian and Asian summer monsoons. As summarized in section 4.1, YD, H1 and D-O stadials are characterized by warm conditions in the tropics and reduced Atlantic THC. This situation leads to an accumulation of salt in the tropical Atlantic which acts as a capacitor eventually yielding to an abrupt resumption of the THC [*Paillard and Labeyrie*, 1994; *Schmidt et al.*, 2004] accompanied by a return to La Niña-like conditions in the tropics and warmer temperatures at high northern latitudes. Here, we hypothesize that this also leads to a reduction of the northern hemisphere ice sheets extent, as logically implied by the observed northward movement of the ITCZ. During the glacial, insolation and ice volume are such that northern ice sheet extent tends to increase again, so that the system moves toward a dominant El Niño-like climatic state again, resulting in millennial oscillations. In contrast, during the last deglaciation, the increase in northern summer insolation finally impedes the growth of northern ice sheets and the system reaches Holocene relatively stable climatic conditions, corresponding to a dominant La Niña-like climatic state.

[29] In summary, we suggest that the combination of rapid changes in atmospheric circulation and water vapor transport induced by SST anomalies in the tropical Pacific on one hand, and of growth of northern hemisphere ice sheets and associated changes in THC over several centuries on the other hand, created an oscillator with millennial time response that operated during the last glacial and deglaciation.

5. Conclusion

[30] SST and $\Delta\delta^{18}O_{sw}$ records from two well-dated Indian Ocean cores covering the last deglaciation period show that salinity increased in the eastern tropical Indian Ocean and Mozambique

Channel area during the H1 (~18 to 14.5 ka) and YD (~13 to 11.5 ka) time intervals. There was thus an increase in salinity along the route of warm surface water transport from the Indian to the Atlantic Ocean during these time periods. As modeling results indicate that progressive warming of the Southern Ocean and gradual retreat of the maximum sea ice extent resulted in an increased mass transport into the Atlantic Ocean after about 18 ka, we conclude that salt transport from the Indian Ocean to the tropical Atlantic Ocean contributed to create the observed accumulation of salt in the tropical Atlantic Ocean during H1. This accumulation of salt and heat in the tropical Atlantic Ocean during H1 and the YD created favorable conditions for an abrupt resumption of the THC and abrupt northern hemisphere warming, when the salt quantity in low-latitude surface and sub-surface waters became sufficient to overcome the antagonist effect of low salinity polar waters at high northern latitudes [*Paillard and Labeyrie*, 1994; *Schmidt et al.*, 2004], as observed at the transition from H1 to the B-A and from the YD to the Holocene.

[31] Moreover, accounting for records of glacial millennial climate variability at high and low latitudes and recent modeling studies, we suggest that the observed pattern of millennial climate variability during the last glacial and deglaciation resulted from the interaction between the relatively slow expansion and decay of northern hemisphere ice sheets, and ENSO variability, through changes in the ITCZ position. This interaction generated an oscillator with millennial time response that operated during glacials and deglaciations only, as its long time response depends on the presence of northern ice sheets and their variable extent.

Acknowledgments

[32] We acknowledge F. Dewilde, G. Isguder, J. Tessier, and B. Lecoat for processing the samples and performing the isotopic measurements as well as S. Godefroy and N. Caillon for assistance with Mg/Ca measurements. We thank M. Paterne for ^{14}C measurements on core MD79-257 and A. Juillet-Leclerc for fruitful discussions. This work was supported by the Pole-Ocean-Pole (EVK-2000-00089) project funded by the European Union, by the CNRS, CEA, and IPEV, as well as by the PNEDC and IMAGES programs. This is contribution 2349 of the LSCE.

References

Alley, R. B., et al. (1993), Abrupt increase in Greenland snow accumulation at the end of the Younger Dryas event, *Nature*, *362*, 527–529.

Bard, E., F. Rostek, and C. Sonzogni (1997), Interhemispheric synchrony of the last deglaciation inferred from alkenone paleothermometry, *Nature*, *385*, 707–710.

Barker, S., M. Greaves, and H. Elderfield (2003), A study of cleaning procedures used for foraminiferal Mg/Ca paleothermometry, *Geochem. Geophys. Geosyst.*, *4*(9), 8407, doi:10.1029/2003GC000559.

Blunier, T., and E. J. Brook (2001), Timing of millennial-scale climate change in Antarctica and Greenland during the last glacial period, *Science*, *291*, 109–112.

Bond, G., et al. (1992), Evidence for massive discharges of icebergs into the North Atlantic Ocean during the last glacial period, *Nature*, *360*, 245–251.

Bond, G., W. Broecker, S. Johnsen, J. McManus, L. Labeyrie, J. Jouzel, and G. Bonani (1993), Correlations between climate records from North Atlantic sediments and Greenland ice, *Nature*, *365*, 143–147.

Broecker, W. S. (1994), Massive iceberg discharges as triggers for global climate change, *Nature*, *372*, 421–424.

Brown, S. J., and H. Elderfield (1996), Variations in Mg/Ca and Sr/Ca rations of planktonic foraminifera caused by post-depositional dissolution: Evidence of shallow Mg-dependent dissolution, *Paleoceanography*, *11*, 543–551.

Cane, M., and A. C. Clement (1999), A role for the tropical Pacific coupled ocean-atmosphere system on Milankovitch and millennial timescales. part II: Global impacts, in *Mechanisms of Global Climate Change at Millennial Time Scales*, *Geophys. Monogr. Ser.*, vol. 112, edited by P. Clark, R. S. Webb, and L. D. Keigwin, pp. 373–383, AGU, Washington, D. C.

Chiang, J. C. H., M. Biasutti, and D. S. Battisti (2003), Sensitivity of the Atlantic Intertropical Convergence Zone to Last Glacial Maximum boundary conditions, *Paleoceanography*, *18*(4), 1094, doi:10.1029/2003PA000916.

Clement, A. C., and M. Cane (1999), A role for the tropical Pacific coupled ocean-atmosphere system on Milankovitch and millennial timescales. part I: A modeling study of tropical Pacific variability, in *Mechanisms of Global Climate Change at Millennial Time Scales*, *Geophys. Monogr. Ser.*, vol. 112, edited by P. Clark, R. S. Webb, and L. D. Keigwin, pp. 363–371, AGU, Washington, D. C.

Clement, A. C., R. Seager, and M. A. Cane (1999), Orbital controls on the El Niño/Southern Oscillation and the tropical climate, *Paleoceanography*, *14*, 441–456.

CLIMAP Project Members (1981), Seasonal reconstructions of the Earth's surface at the Last Glacial Maximum, *Geol. Soc. Am. Map Chart Ser.*, *MC-36*, 1–18.

Conkright, M., S. Levitus, T. O'Brien, T. Boyer, J. Antonov, and C. Stephens (1998), World Ocean Atlas 1998 CD-ROM data set documentation, 16 pp., Natl. Oceanogr. Data Cent., Silver Spring, Md.

Coplen, T. B. (1988), Normalization of oxygen and hydrogen isotope data, *Chem. Geol.*, *72*, 293–297.

de Garidel-Thoron, T., Y. Rosenthal, F. Bassinot, and L. Beaufort (2005), Stable sea surface temperatures in the Western Pacific Warm Pool over the past 1.75million years, *Nature*, *433*, 294–298.

de Villiers, S., M. Greaves, and H. Elderfield (2002), An intensity ratio calibration method for the accurate determination of Mg/Ca and Sr/Ca of marine carbonates by ICP-AES, *Geochem. Geophys. Geosyst.*, *3*(1), 1001, doi:10.1029/2001GC000169.

Dekens, P. S., D. W. Lea, D. K. Pak, and H. J. Spero (2002), Core top calibration of Mg/Ca in tropical foraminifera: Refining paleotemperature estimation, *Geochem. Geophys. Geosyst.*, *3*(4), 1022, doi:10.1029/2001GC000200.

Duplessy, J.-C., P. L. Blanc, and A. W. Bé (1981), Oxygen-18 enrichment of planktonic foraminifera due to gametogenic calcification below the euphotic zone, *Science*, *213*, 1247–1250.

Duplessy, J.-C., E. Bard, M. Arnold, N. J. Shackleton, J. Duprat, and L. Labeyrie (1991), How fast did the ocean-atmosphere system run during the last deglaciation?, *Earth Planet. Sci. Lett.*, *103*, 27–40.

Duplessy, J. C., L. Labeyrie, M. Arnold, M. Paterne, J. Duprat, and T. C. E. van Weering (1992), Changes in surface salinity of the North Atlantic Ocean during the last deglaciation, *Nature*, *358*, 485–487.

Duplessy, J. C., L. Labeyrie, and C. Waelbroeck (2002), Constraints on the ocean oxygen isotopic enrichment between the Last Glacial Maximum and the Holocene: Paleoceanographic implications, *Quat. Sci. Rev.*, *21*, 315–330.

Hays, J. D., J. Imbrie, and N. J. Shackleton (1976), Variations in the Earth's orbit: Pacemaker of the ice ages, *Science*, *194*, 1121–1132.

Heinrich, H. (1988), Origin and consequences of cyclic ice-rafting in the northeast Atlantic Ocean during the past 130000 years, *Quat. Res.*, *29*, 142–152.

Huguet, C., J.-H. Kim, J. S. Sinninghe Damsté, and S. Schouten (2006), Reconstruction of sea surface temperature variations in the Arabian Sea over the last 23 kyr using organic proxies (TEX_{86} and $U^{K'}_{37}$), *Paleoceanography*, *21*, PA3003, doi:10.1029/2005PA001215.

Jouzel, J., et al. (1995), The two-step shape and timing of the last deglaciation in Antarctica, *Clim. Dyn.*, *11*, 151–161.

Khodri, M., Y. Leclainche, G. Ramstein, P. Braconnot, O. Marti, and E. Cortijo (2001), Simulating the amplification of orbital forcing by ocean feedbacks in the last glaciation, *Nature*, *410*, 570–574.

Kienast, M., S. Steinke, K. Stattegger, and S. E. Calvert (2001), Synchronous tropical South China Sea SST change and Greenland warming during deglaciation, *Science*, *291*, 2132–2134.

Knorr, G., and G. Lohmann (2003), Southern Ocean origin for the resumption of Atlantic thermohaline circulation during deglaciation, *Nature*, *424*, 532–536.

Koutavas, A., J. Lynch-Stieglitz, T. M. Marchitto, and J. P. Sachs (2002), El Niño–like pattern in ice age tropical Pacific sea surface temperature, *Science*, *297*, 226–230.

Kukla, G. J., A. C. Clement, M. A. Cane, and J. E. Gavin (2002), Last interglacial and early glacial ENSO, *Quat. Res.*, *58*, 27–31.

Labeyrie, L. (2000), Glacial climate instability, *Science*, *290*, 1905–1907.

Labeyrie, L., H. Leclaire, C. Waelbroeck, E. Cortijo, J.-C. Duplessy, L. Vidal, M. Elliot, B. Lecoat, and G. Auffret (1999), Insolation forcing and millennial scale variability of the north west Atlantic Ocean: Surface versus deep water changes, in *Mechanisms of Global Climate Change at Millennial Time Scales*, *Geophys. Monogr. Ser.*, vol. 112, edited by P. Clark, R. S. Webb, and L. D. Keigwin, pp. 77–98, AGU, Washington, D. C.

Labeyrie, L., J. Jouzel, C. Lévi, and E. Cortijo (2004), Changements abrupts dans un monde glaciaire, *C. R. Geosci.*, *336*, 721–732.

Lambeck, K., and J. Chappell (2001), Sea level change through the last glacial cycle, *Science*, *292*, 679–686.

Lea, D. W., D. K. Pak, and H. J. Spero (2000), Climate impact of late Quaternary equatorial Pacific sea surface temperature variations, *Science*, *289*, 1719–1924.

Lea, D. W., D. K. Pak, L. C. Peterson, and K. A. Hughen (2003), Synchroneity of tropical and high-latitude Atlantic temperatures over the last glacial termination, *Science*, *301*, 1361–1364.

Levi, C. (2003), Etude des variations climatiques de la zone Indo-Pacifique: Rôle des basses latitudes dans la variabilité millénaire du climat, Ph.D. thesis, 153 pp., Univ. Paris XI, Orsay, France.

Martinez, J. I., L. Taylor, P. De Deckker, and T. Barrows (1998), Planktonic foraminifera from the eastern Indian Ocean: Distribution and ecology in relation to the Western Pacific Warm Pool (WPWP), *Mar. Micropaleontol.*, *34*, 121–151.

Meese, D. A., A. J. Gow, R. B. Alley, G. A. Zielinski, P. M. Grootes, M. Ram, K. C. Taylor, P. A. Mayewski, and J. F. Bolzan (1997), The Greenland Ice Sheet Project 2 depth-age scale: Methods and results, *J. Geophys. Res.*, *102*, 26,411–26,424.

Ostermann, D. R., and W. B. Curry (2000), Calibration of stable isotopic data: An enriched $\delta^{18}O$ standard used for source gas mixing detection and correction, *Paleoceanography*, *15*, 353–360.

Paillard, D., and L. Labeyrie (1994), Role of the thermohaline circulation in the abrupt warming after Heinrich events, *Nature*, *372*, 162–164.

Palmer, M. R., and P. N. Pearson (2003), A 23000-year record of surface water pH and pCO_2 in the western equatorial Pacific Ocean, *Nature*, *300*, 480–482.

Parrenin, F., F. Remy, C. Ritz, M. J. Siegert, and J. Jouzel (2004), New modeling of the Vostok ice flow line and implication for the glaciological chronology of the Vostok ice core, *J. Geophys. Res.*, *109*, D20102, doi:10.1029/2004JD004561.

Peterson, L. C., G. H. Haug, K. A. Hughen, and U. Röhl (2000), Rapid changes in the hydrologic cycle of the tropical Atlantic during the last glacial, *Science*, *290*, 1947–1951.

Philander, S. G. (1990), *El Nino, La Nina, and the Southern Oscillation*, 293 pp., Elsevier, New York.

Prell, W. L. (1985), The stability of low-latitude sea-surface temperatures: An evaluation of the CLIMAP reconstruction with emphasis on the positive SST anomalies, report, 60 pp., U.S. Dep. of Energy, Washington, D. C.

Rind, D. (2000), Relating paleoclimate data and past temperature gradients: Some suggestive rules, *Quat. Sci. Rev.*, *19*, 381–390.

Ropelewski, C. F., and M. S. Halpert (1987), Global and regional scale precipitation patterns associated with the El Nino/Southern Oscillation, *Mon. Weather Rev.*, *115*, 1606–1626.

Rosenthal, Y., and G. P. Lohmann (2002), Accurate estimation of sea surface temperatures using dissolution-corrected calibrations for Mg/Ca paleothermometry, *Paleoceanography*, *17*(3), 1044, doi:10.1029/2001PA000749.

Rosenthal, Y., D. W. Oppo, and B. K. Linsley (2003), The amplitude and phasing of climate change during the last deglaciation in the Sulu Sea, western equatorial Pacific, *Geophys. Res. Lett.*, *30*(8), 1428, doi:10.1029/2002GL016612.

Rühlemann, C., S. Mulitza, P. J. Müller, G. Wefer, and R. Zahn (1999), Warming of the tropical Atlantic Ocean and slowdown of the thermohaline circulation during the last deglaciation, *Nature*, *402*, 511–514.

Salvignac, M. E. (1998), *Variabilité Hydrologique et Climatique Dans l'Océan Austral au Cours du Quaternaire Terminal*, 354 pp., Univ. de Bordeaux I., Bordeaux, France.

Schmidt, G. A., H. J. Spero, and D. W. Lea (2004), Links between salinity variation in the Caribbean and North Atlantic thermohaline circulation, *Nature*, *428*, 160–163.

Schrag, D. P., J. F. Adkins, K. McIntyre, J. L. Alexander, D. A. Hodell, C. D. Charles, and J. F. McManus (2002), The oxygen isotopic composition of seawater during the Last Glacial Maximum, *Quat. Sci. Rev.*, *21*, 331–342.

Shackleton, N. J. (1974), Attainment of isotopic equilibrium between ocean water and benthonic foraminifera genus *Uvigerina*: Isotopic changes in the ocean during the last glacial, in *Les Méthodes Quantitatives d'Étude des Variations du Climat au Cours du Pleistocène*, pp. 203–209, Cent. Natl. Rech. Sci., Gif-sur-Yvette, France.

Sicre, M. A., L. Labeyrie, U. Ezat, J. Duprat, J. L. Turon, S. Schmidt, E. Michel, and A. Mazaud (2005), Mid-latitude southern Indian Ocean response to Northern Hemisphere Heinrich events, *Earth Planet. Sci. Lett.*, *240*, 724–731.

Sonzogni, C., E. Bard, and F. Rostek (1998), Tropical sea-surface temperatures during the last glacial period: A view based on alkenones in Indian Ocean sediments, *Quat. Sci. Rev.*, *17*, 1185–1201.

Stott, L., C. Poulsen, S. Lund, and R. Thunell (2002), Super ENSO and global climate oscillations at millennial time scales, *Science*, *297*, 222–226.

Stuiver, M., and T. F. Braziunas (1993), Sun, ocean, climate and atmospheric $^{14}CO_2$: An evaluation of causal and spectral relationship, *Holocene*, *3*, 289–305.

Stuiver, M., P. J. Reimer, and E. Bard (1998), INTERCAL98 radiocarbon age calibration, 24 000–0 cal BP, *Radiocarbon*, *40*, 1041–1083.

Visser, C., R. Thunell, and L. Stott (2003), Magnitude and timing of temperature change in the Indo-Pacific Warm Pool during deglaciation, *Nature*, *421*, 152–155.

Waelbroeck, C., L. Labeyrie, E. Michel, J. C. Duplessy, J. McManus, K. Lambeck, E. Balbon, and M. Labracherie (2002), Sea-level and deep water temperature changes derived from benthic foraminifera isotopic records, *Quat. Sci. Rev.*, *21*, 295–305.

Waelbroeck, C., S. Mulitza, H. Spero, T. Dokken, T. Kiefer, and E. Cortijo (2005), A global compilation of late Holocene planktonic foraminiferal $\delta^{18}O$: Relationship between surface water temperature and $\delta^{18}O$, *Quat. Sci. Rev.*, *24*, 853–868.

Waelbroeck, C., C. Levi, J.-C. Duplessy, L. Labeyrie, E. Michel, E. Cortijo, F. Bassinot, and F. Guichard (2006), Distant origin of circulation changes in the Indian Ocean during the last deglaciation, *Earth Planet. Sci. Lett.*, *243*, 244–251.

Wang, L. (2000), Isotopic signals in two morphotypes of Globigerinoides ruber (white) from the South China Sea: Implications for monsoon climate change during the last glacial cycle, *Palaeogeogr. Palaeoclimatol. Palaeoecol.*, *161*, 381–394.

Wang, X., A. S. Auler, R. L. Edwards, H. Cheng, P. S. Cristalli, P. L. Smart, D. A. Richards, and C.-C. Shen (2004), Wet periods in northeastern Brazil over the past 210 kyr linked to distant climate anomalies, *Nature*, *432*, 740–743.

Wang, Y. J., H. Cheng, R. L. Edwards, Z. S. An, J. Y. Wu, C.-C. Shen, and J. A. Dorale (2001), A high-resolution absolute-dated Late Pleistocene monsoon record from Hulu Cave, China, *Science*, *294*, 2345–2348.

Weldeab, S., R. R. Schneider, and M. Kölling (2006), Comparison of foraminiferal cleaning procedures for Mg/Ca paleothermometry on core material deposited under varying terrigenous-input and bottom water conditions, *Geochem. Geophys. Geosyst.*, *7*, Q04P12, doi:10.1029/2005GC000990.

Zhang, R., and T. L. Delworth (2005), Simulated tropical response to a substantial weakening of the Atlantic thermohaline circulation, *J. Clim.*, *18*, 1853–1860.